Article

Nitric Oxide Interaction with Cytochrome *c*‘ and Its Relevance to Guanylate Cyclase. Why Does the Iron Histidine Bond Break?

Marcelo A. Mart, Luciana Capece, Alejandro Crespo, Fabio Doctorovich, and Dario A. Estrin

J. Am. Chem. Soc., **2005**, 127 (21), 7721-7728• DOI: 10.1021/ja042870c • Publication Date (Web): 05 May 2005

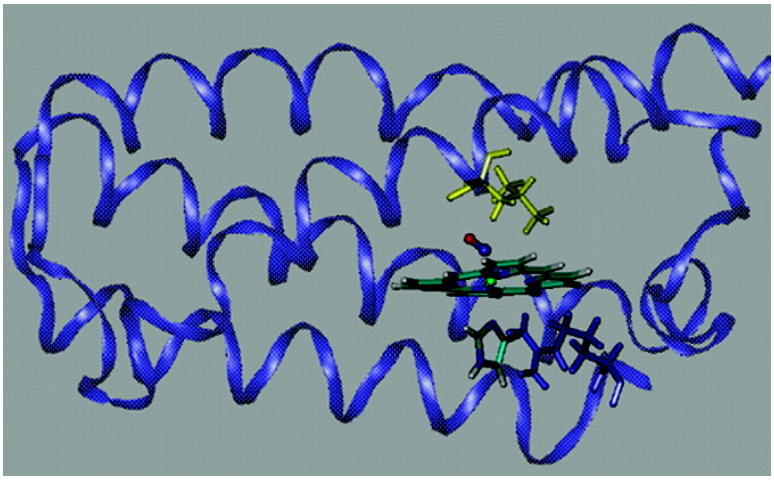

More About This Article

Additional resources and features associated with this article are available within the HTML version:

- Supporting Information
- Links to the 8 articles that cite this article, as of the time of this article download
- Access to high resolution figures
- Links to articles and content related to this article
- Copyright permission to reproduce figures and/or text from this article

View the Full Text HTML

J|A|C|S
ARTICLES
Published on Web 05/05/2005

Nitric Oxide Interaction with Cytochrome *c*′ and Its Relevance to Guanylate Cyclase. Why Does the Iron Histidine Bond Break?

Marcelo A. Martí, Luciana Capece, Alejandro Crespo, Fabio Doctorovich, and Dario A. Estrin*

Contribution from the Departamento de Química Inorgánica, Analítica y Química Física/ INQUIMAE-CONICET, Facultad de Ciencias Exactas y Naturales, Universidad de Buenos Aires, Ciudad Universitaria, Pabellón II, Buenos Aires (C1428EHA), Argentina

Received November 25, 2004; Revised Manuscript Received March 9, 2005; E-mail: dario@qi.fcen.uba.ar

Abstract: Soluble guanylate cyclase (sGC), the mammalian receptor for nitric oxide (NO), is a heme protein with a histidine as the proximal ligand. Formation of a five-coordinate heme−NO complex with the associated Fe−His bond cleavage is believed to trigger a conformational change that activates the enzyme and transduces the NO signal. Cytochrome *c*′ (cyt *c*′) is a protobacteria heme protein that has several similarities with sGC, including the ability to form a five-coordinate NO adduct and the fact that it does not bind oxygen. Recent crystallographic characterization of cyt *c*′ from *Alcaligenes xylosoxidans* (AXCP) has yielded the discovery that exogenous ligands are able to bind to the Fe center from either side of the porphyrin plane. In this paper, we explore the molecular basis of the NO interaction with AXCP using hybrid quantum-classical simulation techniques. Our results suggest that Fe−His bond breaking depends not only on the iron−histidine bond strength but also on the existence of a local minimum conformation of the protein with the histidine away from the iron. We also show that AXCP is a useful paradigm for NO interaction with heme proteins, particularly regarding the activation/deactivation mechanism of sGC. The results presented here fully support a recently proposed model of sGC activation in which NO is not only the iron ligand but also catalyzes the activation step.

Introduction

The mammalian receptor for nitric oxide (NO) is the soluble form of guanylate cyclase (sGC).[1] sGC is a heterodimeric heme protein composed of α and β subunits. Structure−function studies on sGC have been hampered by the lack of detailed structural information on the NO binding domain. It is accepted that the ferrous heme is linked to the β subunit via a histidine (His) residue (H105 in rat, human, and bovine sGC).[2] However, there is still some controversy regarding the distal pocket polarity and the ferrous sGC resting state. Depending on the isolation procedure, resonance Raman spectroscopy revealed two different heme pocket environments for sGC (termed sGC_1 and sGC_2).[3] For sGC_1, which is obtained with substoichiometric heme content and is loaded with heme for spectroscopic measurements,[4] the resting state has been proposed to be a mainly hexacoordinated (6c) His−Fe−His low spin configuration.[3,5] On the other hand, sGC_2, which is obtained highly loaded with heme,[6,7] displays spectral properties indicative of a high spin pentacoordinated (5c) His−Fe complex resting state and a CO adduct indicative of a negatively polarizing environment.[8,9] Recently, the crystal structure of the heme domain of a protein from *Thermoanaerobacter tengcogensis* (TtTar4H), significantly homologous to sGC, has been obtained.[10] The spectroscopic characterization of this and another sGC homologue protein from *Vibrio cholerae* (VCA0720) revealed that both proteins exhibit 5c His−Fe high spin resting state configurations, similarly to that found in sGC_2.[11] In sGC, formation of a thermodynamically stable 5c-NO heme complex upon NO binding, with the associated Fe−His bond cleavage, is believed to be the trigger of a conformational change that activates the enzyme and transduces the NO signal.[12] However, there is still a debate about the precise role played by NO in the activation mechanism. On the basis of the analysis of kinetic data, Marletta et al. argued that NO is involved not only as the

(1) Moncada, S.; Palmer, R. M.; Higgs, E. A. *Pharmacol. Rev.* **1991**, *43*, 109−142.
(2) Zhao, Y.; Schelvis, J. P.; Babcock, G. T.; Marletta, M. A. *Biochemistry* **1998**, *37*, 4504−4509.
(3) Vogel, K. M.; Hu, S.; Spiro, T. G.; Dierks, E. A.; Yu, A. E.; Burstyn, J. N. *J. Biol. Inorg. Chem.* **1999**, *4*, 804−813.
(4) Yu, A. E.; Hu, S.; Spiro, T. G.; Burstyn, J. N. *J. Am. Chem. Soc.* **1994**, *116*, 4117−4118.
(5) Burstyn, J. N.; Yu, A. E.; Dierks, E. A.; Hawkins, B. K.; Dawson, J. H. *Biochemistry* **1995**, *34*, 3896−5903.
(6) Denium, G.; Stone, J. R.; Babcock, G. T.; Marletta, M. A *Biochemistry* **1996**, *35*, 1540−1547.
(7) Tomita, T.; Ogura, T.; Tsuyama, S.; Imai, Y.; Kitagawa, T. *Biochemistry* **1997**, *36*, 10155−10160.
(8) Li, Z.; Pal, B.; Takenaka, S.; Tsuyama, S.; Kitagawa, T. *Biochemistry* **2005**, *44*, 939−946.
(9) Kim, S.; Deinum, G.; Gardner, M. T.; Marletta, M. A.; Babcock, G. T. *J. Am. Chem. Soc.* **1996**, *118*, 8769−8770.
(10) Pellicena, P.; Karow, D. S.; Boon, E. M.; Marletta, M. A.; Kuriyan, J. *Proc. Natl. Acad. Sci. U.S.A.* **2004**, *101*, 35, 12854−12859.
(11) Karow, D. S.; Pan, D.; Tran, R.; Pellicena, P.; Presley, A.; Mathies, R. A.; Marletta, M. A *Biochemistry* **2004**, *43*, 10203−10211.
(12) Denninger, J. W.; Marletta, M. A. *Biochim. Biophys. Acta* **1999**, *1411*, 334−350.

heme group ligand but that it also participates as a catalyst in the 6c-NO (inactive) to 5c-NO (active) transition.[13,14] However, Bellamy et al.,[15] based on the same results, showed that it is unnecessary to assume that NO is involved in the 6c-NO to 5c-NO transition and that the experimental results are consistent with a simpler model of sGC activation with a single NO binding event.[15]

Cytochromes *c*′ (cyt *c*′) are a distinct family of class II cytochromes found in the periplasm of certain denitrifying, photosynthetic, methanotrophic, and sulfur-oxidizing bacteria.[16] Unlike most *c*-type cytochromes, the heme group is attached to the C-terminus of a four α helix bundle, and it contains only a single axial ligand resulting in a 5c Fe−His center. In contrast, a 6c His−Fe−Met heme is observed for the electron transport cytochrome *c* proteins. Although the exact physiological role of cyt *c*′ is unclear, several studies have suggested that NO binding to the heme may help bacteria to suppress potentially toxic levels of free NO.[17] In particular, Moir and co-workers have shown that a cyt *c*′ deficient mutant of *Rhodobacter capsulatus* exhibited increased sensitivity to nitrosative stress[18] and suggested that cyt *c*′ might function as an NO reductase.[19]

Additional interest in the coordination chemistry of cyt *c*′ stems from similarities with sGC, including the ability to form a 5c-NO adduct. Recent crystallographic characterization of cyt *c*′ from *Alcaligenes xylosoxidans* (AXCP) has yielded the discovery that exogenous ligands are able to bind to the Fe center from either side of the heme plane.[20] Whereas the 6c-CO complex contains the CO bound at the distal side, the 5c-NO adduct exhibits proximal coordination geometry with NO residing at the site originally occupied by the proximal His ligand and the Fe−His bond broken.[20] Further similarities between AXCP and sGC are the fact that both form 6c-NO intermediates with the proximal Fe−His bond intact and the NO at the distal side[6,21,22] and the fact that none of them bind oxygen.[14,23] Clearly, the novel proximal coordinated heme−NO moiety in AXCP has potential implications for understanding sGC activation mechanism. In this context, cyt *c*′ has been put forward as a structural model for the NO binding domain of sGC, motivating several investigations in the last few years.[14,24−28] Differential effects of NO and CO on the activation of sGC have been explained through X-ray crystallography of cyt *c*′ complexes.[20] The existence of a 6c-NO intermediate was investigated by Andrew et al. using stopped-flow measurements.[22,27] Flash photolysis experiments have been performed to investigate the NO release mechanism.[19] Resonance Raman investigations have been carried out to analyze the environment of NO and CO in the corresponding 5c and 6c complexes.[26]

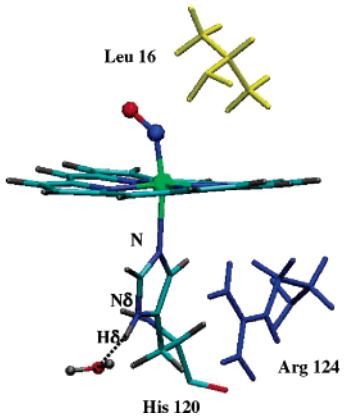

Figure 1. 6c-NO complex in AXCP.

Structural and spectroscopic information about 6c-NO porphyrin complexes has been obtained by employing synthetic models. These systems display a strong structural negative trans effect, consisting of a significant lengthening of the Fe−N bond trans to the NO of 0.15−0.25 Å, with the concomitant weakening of the bond.[29] However, the proximal Fe−His bond in the 6c-NO complex does not break in all heme proteins. Some proteins, such as myoglobin, horseradish peroxidase (HRP), and the hemoglobin β (Hb β) chain, remain 6c, whereas others such as Fix-L (an oxygen sensor protein that changes conformation upon oxygen binding to the heme),[30] hemoglobin α-chain (Hb α), sGC, and also AXCP form 5c-NO complexes.[31] We have shown in a previous work that the Fe−His bond strength depends mainly on the His capacity to donate charge to the heme Fe^{2+} ion (σ donation capacity), which is correlated to the H-bonding to the His Hδ (the hydrogen atom bonded to the Nδ atom of the imidazole ring, as depicted in Figure 1).[32] The Fe−His bond strength can be conveniently monitored by measuring the Raman resonance frequency corresponding to the Fe−N stretching band. It has been argued that proteins forming 5c-NO adducts as Fix-L, sGC, or Hbα exhibit Fe−N stretching frequencies below 210 cm^{-1}, whereas proteins forming 6c-NO complexes show Fe−His stretching values in the 220−240 cm^{-1} range.[31] It is interesting to note that in AXCP, despite the fact that it forms a 5c-NO complex and that the Fe−His bond breaks, a 231 cm^{-1} value has been reported for the Fe−His stretching frequency.[26] Andrew et al.[26] suggested that the high frequency of the Fe−His bond could be due to a deprotonated His residue and that NO binding and protonation of the His residue could lead to breaking of the Fe−His bond.

(13) Ballou, D. P.; Zhao, Y.; Brandish, P. E.; Marletta, M. A. *Proc. Natl. Acad. Sci. U.S.A.* **2002**, *99*, 12097−12101.
(14) Zhao, Y.; Brandish, P. E.; Ballou, D. P.; Marletta, M. A. *Proc. Natl. Acad. Sci. U.S.A.* **1999**, *96*, 14753−14758.
(15) Bellamy, T. C.; Wood, J.; Garthwaite, J. *Proc. Natl. Acad. Sci. U.S.A.* **2002**, *99*, 507−510.
(16) (a) Meyer, T. E.; Kamen, M. D. *Adv. Protein. Chem.* **1982**, *35*, 105−212. (b) Iwasaki, H.; Yoshimura, T.; Suzuki, S.; Shidara, S. *Biochim. Biophys. Acta* **1991**, *1058*, 79−82. (c) Schnidt, T. M.; DiSpirito, A. A. *Arch. Microbiol.* **1990**, *154*, 453−458.
(17) Moir, J. W. B. *Biochim. Biophys. Acta* **1999**, *1430*, 65−72.
(18) Cross, R.; Aish, J.; Patson, S. J.; Poole, R. K.; Moir, J. W. B *J. Bacteriol.* **2000**, *182*, 1442−1447.
(19) Cross, R.; Lloyd, D.; Poole, R. K.; Moir, J. W. B. *J. Bacteriol.* **2001**, *183*, 3050−3054.
(20) Lawson, D. M.; Stevenson, C. E. M.; Andrew, C. R.; Eady, R. R. *EMBO J.* **2000**, *19*, 5661−5671.
(21) Makino, R.; Matsuda, H.; Obayashi, E.; Shiro, Y.; Iizuka, T.; Hori, H. *J. Biol. Chem.* **1999**, *274*, 7714−7723.
(22) George, J. S.; Andrew, C. R.; Lawson, D. M.; Thorneley, R. N. F.; Eady, R. R. *J. Am. Chem. Soc.* **2001**, *123*, 9683−9684.
(23) Stone, J. R.; Marletta, M. A. *Biochemistry* **1994**, *33*, 5636−5640.
(24) Lawson, D. M.; Stevenson, C. E. M.; Andrew, C. R.; George, S. J.; Eady, R. R. *Biochem. Soc. Trans.* **2003**, *31*, 553−557.
(25) Andrew, C. R.; Green, E. L.; Lawson, D. M.; Eady, R. R. *Biochemistry* **2001**, *40*, 4115−4122.
(26) Andrew, C. R.; George, S. J.; Lawson, D. M.; Eady, R. R. *Biochemistry* **2002**, *41*, 2353−2360.
(27) Andrew, C. R.; Rodgers, K. R.; Eady, R. R. *J. Am. Chem. Soc.* **2003**, *125*, 9548−9549.
(28) Mayburd, A. L.; Kassner, R. J. *Biochemistry* **2002**, *41*, 11582−11591.
(29) Wyllie, G. R. A.; Schulz, C. E.; Scheidt, W. R. *Inorg. Chem.* **2003**, *42*, 5722−5734.
(30) Gong, W.; Hao, B.; Mansy, S. S.; Gonzalez, G.; Gilles-Gonzalez, M. A.; Chan, M. K. *Proc. Natl. Acad. Sci. U.S.A.* **1998**, *95*, 15177−15182.
(31) Schelvis, J. P. M.; Seibold, S. A.; Cerda, J. F.; Garavito, R. M.; Babcock, G. T. *J. Phys. Chem. B* **2000** *104*, 10844−10850.
(32) (a) Martí, M. A.; Scherlis, D. A.; Doctorovich, F. A.; Ordejón, P.; Estrin, D. A. *J. Biol. Inorg. Chem.* **2003**, *6*, 595−600. (b) Scherlis, D. A.; Martí, M. A.; Ordejón, P.; Estrin, D. A. *Int. J. of Quantum Chem.* **2002**, *90*, 1505−1514.

In this paper, we provide computational evidence suggesting that Fe−His bond breaking depends not only on the Fe−His bond strength but also on the existence of a local minimum conformation of the protein with the proximal His away from the iron. Our results also show that AXCP is a useful paradigm for NO interaction with heme proteins and particularly regarding the activation/deactivation mechanism of sGC. The results also shed light into some details of AXCP chemical properties and function.

Computational Methods

We constructed initial structures for our calculations from the structure of the nitric oxide complex of the AXCP from *A. xylosoxidans* (PDB code 1E85).[20] Histidine protonation was assigned favoring H-bond formation. The system was solvated with water molecules up to a distance of 30 Å of the heme center. The final system consisted of 2805 waters and 1790−1800 protein atoms. All classical simulations were performed with the NAMD package[33] with the Amber force field.[34] The whole system was heated to 300 K, and 400 ps molecular dynamics was performed to allow the system to relax and equilibrate. Then, the system was cooled slowly to 0 K. This process was followed by full hybrid quantum-classical (QM-MM) geometry optimizations using a conjugate gradient algorithm. Only residues located less than 10 Å apart from the catalytic center were allowed to move freely in the QM-MM runs. Calculations of the isolated QM system in a vacuum were also performed to assess the relevance of the protein environment effects.

All QM computations were performed at the density functional theory (DFT) level with the SIESTA code.[35] DFT methods, including the SIESTA code, have shown an excellent performance for medium and large systems and have also proven to be appropriate for biomolecules and, specifically, for heme models.[32,36] The use of standard norm-conserving pseudo-potentials[37] avoids the computation of core electrons, smoothing at the same time the valence charge density. In our study, the nonlinear partial-core correction[38] is applied to the iron atom. Basis functions consist of localized (numerical) pseudo-atomic orbitals, projected on a real space grid to compute the Hartree potential and exchange correlation potential matrix elements. For all atoms, basis sets of double plus polarization quality were employed, with a pseudo-atomic orbital energy shift of 25 meV and a grid cutoff of 150 Ry.[35] Calculations were performed using the generalized gradient approximation functional proposed by Perdew et al.[39] This combination of functional, basis sets, and grid parameters has been already validated for heme models.[32] The classical subsystem was treated using the parametrization from the AMBER force field.[34]

We have selected the heme group plus the relevant ligands as the quantum subsystem. The rest of the protein unit mentioned previously and the water molecules were treated classically. The frontier between the QM and MM portions of the system has been treated by the scaled position link atom method[40] adapted to our SIESTA code. Link atoms have been used in the proximal His to separate the QM treated imidazol ring from the backbone of the amino acids and to separate the core of the heme from the side chains. The ferrous 5c-His heme group isolated or in the protein was treated as a high spin (HS) quintuplet state, which is known to be the ground state for this system.[41] The 5c- or 6c-NO ferrous heme groups were treated as low spin (LS) states, which are known to be the ground state for these systems.[41] More technical details about the QM-MM implementation can be found elsewhere.[42]

Scheme 1. Proposed Mechanism[13,14] for the Activation of sGC[a]

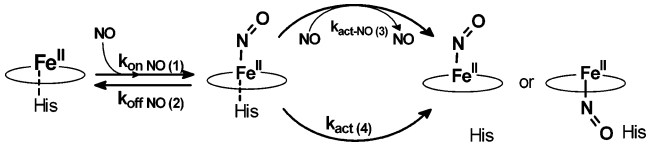

[a] In the conversion of the 6c species to the 5c-NO heme complex (reaction 3), NO acts as a catalyst, as it is not consumed. Uncatalyzed conversion (reaction 4) does not involve NO. The final structure shows sGC 5c-NO with NO on either side of the heme.

Ligand affinities (EL) were calculated as

$$E_L = E_{Enz-L} - E_L - E_{Enz}$$

where E_{Enz-L} is the energy of the ligand bound enzyme, E_{Enz} is the energy of the ligand free enzyme, and E_L is the energy of the isolated ligand.

Obtaining accurate free energy profiles and thus taking into account entropic effects requires an extensive sampling, which is very difficult to achieve at the DFT QM-MM level. For these reasons, we have computed the potential energy profiles using restrained energy minimizations along the selected reaction paths. For this purpose, an additional term is added to the potential energy according to $V(\xi) = k(\xi - \xi_0)^2$, where k is an adjustable force constant, ξ is the value of the reaction coordinate in the system's particular configuration, and ξ_0 is the reaction coordinate desired value. Varying ξ_0, the system is forced to follow the minimum reaction path along the given coordinate. This method has been successfully applied in the QM-MM reaction path calculations.[42]

Results and Discussion

There has been recently much debate about the molecular basis for the activation mechanism of sGC by NO.[13−15] In this context, the similarity of the spectroscopic and kinetic behavior of sGC and AXCP makes AXCP a useful model for understanding the molecular basis of heme proteins and particularly sGC interaction with NO. As mentioned in the Introduction, Marletta's group proposed that two molecules of NO participate in sGC activation mechanism, according to Scheme 1.[13,14] The corresponding obtained rate constant values were $1 \times 10^8\ M^{-1}\ s^{-1}$ for k_{onNO}, $2.4 \times 10^5\ M^{-1}\ s^{-1}$ for k_{act-NO}, and $5 \times 10^{-4}\ s^{-1}$ for k_{act}.

The simpler mechanism supported by the analysis of Bellamy et al.[15] is a subset of the one shown in Scheme 1 that excludes reaction 3 and therefore makes the activation step independent of NO (through reaction 4). The experimental value obtained for k_{onNO} is similar to that obtained by Marletta's group; however, the value obtained for k_{act} was $1.3\ s^{-1}$, which is significantly higher. To assess the feasibility of this mechanism

(33) Kaole, L.; Skeel, R.; Bhandarkar, M.; Brunner, R.; Gursoy, A.; Krawetz, N.; Phillips, J.; Shinozaki, A.; Varadarajan, K.; Shulten, K. *J Comput. Phys.* **1999**, *151*, 283−312.
(34) Pearlman, D. A.; Case, D. A.; Caldwell, J. W.; Ross, W. R.; Cheatham, T. E., III; DeBolt, S.; Ferguson, D.; Seibel, G.; Kollman, P. *Comput. Phys. Commun.* **1995**, *91*, 1−41. (b) Cornell, W. D.; Cieplak, P.; Bayly, C. I.; Gould, I. R.; Merz, K. M., Jr.; Ferguson, D. M.; Spellmeyer, D. C.; Fox, T.; Caldwell, J. W.; Kollman, P. A. *J. Am. Chem. Soc.* **1995**, *117*, 5179−5197. (c) Wang, J.; Cieplak, P.; Kollman, P. A. *J. Comput. Chem.* **2000**, *21*, 1049−1074.
(35) Soler, J. M.; Artacho, E.; Gale, J.; García, A.; Junquera, J.; Ordejón, P.; Sánchez-Portal, D. *J. Phys. Cond. Matt.* **2002**, *14*, 2745−2779.
(36) (a) Martí, M. A.; Crespo, A.; Bari, S. E.; Doctorovich, F. A.; Estrin, D. A. *J. Phys. Chem. B* **2004**, *108*, 18073−18080. (b) Guallar, V.; Friesner, R. A. *J. Am. Chem. Soc.* **2004**, *126*, 8501−8508. (c) Schoneboom, J. C.; Lin, H.; Reuter, N.; Thiel, W.; Cohen, S.; Ogliaro, F.; Shaik, S. *J. Am. Chem. Soc.* **2002**, *124*, 8142−8151.
(37) Troullier, N.; Martins, J. L. *Phys. Rev. B* **1991**, *43*, 1993−2006.
(38) Louie, S. G.; Froyen, S.; Cohen, M. L. *Phys. Rev. B* **1982**, *26*, 1738−1742.
(39) Perdew, J. P.; Burke, K.; Ernzerhof, M. *Phys. Rev. Lett.* **1996**, *77*, 3865−3868.
(40) (a) Eichinger, M.; Tavan, P.; Hutter, J.; Parrinello, M. *J. Chem. Phys.* **1999**, *110*, 10452−10467. (b) Rovira, C.; Schultze, B.; Eichinger, M.; Evanseck, J. D.; Parrinello, M. *Biophys. J.* **2001**, *81*, 435−445.
(41) Rovira, C.; Kunc, K.; Hutter, J.; Ballone, P.; Parrinello, M. *J. Phys. Chem. A* **1997**, *101*, 8914−8925.
(42) Crespo, A.; Scherlis, D. A.; Martí, M. A.; Ordejón, P.; Roitberg, A. E.; Estrin, D. A. *J. Phys. Chem. B* **2003**, *107*, 13728−13736.

Table 1. Structural Optimized Parameters[a] (Å and deg) for the 6c-NO complex in AXCP (Protein), for an Isolated 6c-NO Complex in a Vacuum (without the Protein and Heme Side Chains), as Compared to Experimental Data for Fe Tetraphenylporphyrin 1-Methylimidazole NO Complex[29]

	protein	vacuum	expt[29]
dFe−NO (Å)	1.74	1.75	1.75
dN−O (Å)	1.21	1.21	1.18
Fe−N−O angle (deg)	136.9	138.7	137.7
dFe−N_{His} (Å)	2.33	2.24	2.17
dFe−N_{His}(NO free) (Å)	2.18	2.16	
Δq_{His} (*e*)	0.080	0.121	
Δq_{NO} (*e*)	−0.071	−0.046	

[a] Δq_{His} and Δq_{NO} (*e*) represent the amount of charge donated and received by His and NO, respectively.

for AXCP, we have analyzed the relevant steps by performing QM-MM optimizations of reactants and products and also by computing potential energy profiles.

Structural Characteristics of the 6c-His−Fe−NO Complex in AXCP. The species formed upon NO addition to AXCP (reaction 1), calculated to be the 6c His−Fe−NO complex with NO at the distal position, corresponds to a local minimum structure. To check the reliability of the QM-MM optimization, which may present flaws if there are large protein conformational changes, we obtained the 6c-NO complex employing two different starting structures: the experimental 6c-CO complex in which CO was replaced by NO and a starting structure constructed from the experimental 5c-NO structure with NO in the proximal side in which the proximal NO is replaced by a NO coordinated to the distal side. In the latter case, we have first performed a potential energy profile calculation for the Fe−His distance, to locate the local minimum corresponding to the 6c structure with the Fe−His bond present. Both QM-MM optimizations yielded the same optimized 6c-NO structure. The 6c-NO species has been experimentally characterized by resonance Raman spectroscopy.[26] Figure 1 shows the corresponding QM-MM optimized structure. Relevant structural parameters for the complex in the protein and in a vacuum are presented in Table 1.

The data presented in Table 1 are typical for a {FeNO}^{7} species according to the Enemark and Feltham[43] notation. The Fe−N−O angle is slightly smaller in the protein than in the isolated complex, probably due to the stereochemically unfavorable interaction with Leu 16.

The negative NO trans effect (that produces a weakening of the Fe−His bond) is evidenced in the longer value for this bond in the 6c-NO complex as compared to that in the 5c-His complex.

Conversion of 6c-NO to 5c-NO Species. The 6c-NO species has been shown to be short-lived in AXCP. The X-ray structure of nitrosyl AXCP shows NO present at the proximal side, with the corresponding proximal Fe−His bond broken and the His residue interacting with Arg 124. As mentioned previously, there seems to be an inconsistency between the high Raman frequency of the Fe−His bond (ν_{Fe-His}) in AXCP (231 cm^{-1}) and the fact that the bond breaks.[27] In a previous work, we showed that ν_{Fe-His} is correlated to the Fe−His bond dissociation energy (ΔE_{Fe-His}) and the amount of σ-donation from the His to the metal (Δq_{His}) obtained by QM or QM-MM calculations.[32] Figure 2 shows plots of experimental ν_{Fe-His} versus computed ΔE_{Fe-His} and Δq_{His} for four different heme proteins and AXCP.

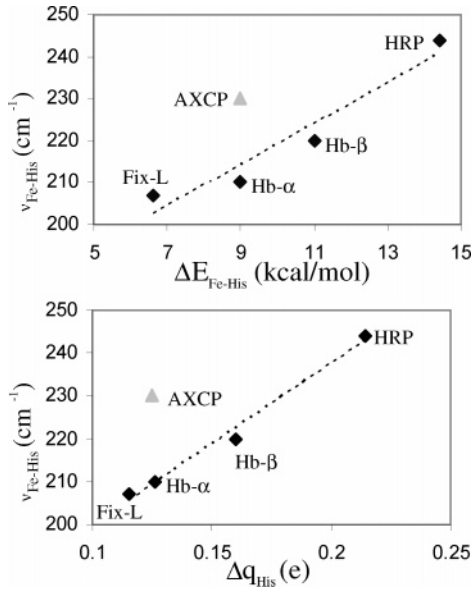

Figure 2. Plots of the experimental ν_{Fe-His} (cm^{-1}) vs computed ΔE_{Fe-His} (upper panel) and vs computed Δq_{His} (lower panel). Black diamonds represent values for the following heme proteins: Hb-α ν_{Fe-His} 207 cm^{-1}, Fix-L 210 cm^{-1}, Hb-β 220 cm^{-1}, and HRP 244 cm^{-1} taken from refs 23 and 24. AXCP values are represented by gray triangles.[17]

As it can be seen from the plot, the experimental value for AXCP ν_{Fe-His} (231 cm^{-1})[26] does not follow the observed correlation for the other heme proteins. Both the computed ΔE_{Fe-His} and Δq_{His} values for AXCP point to a neutral His, similar to that found in Fix-L (a protein that also forms a 5c-NO complex). Heme proteins with high ν_{Fe-His} frequencies such as HRP or Hb-β (that form 6c-His−Fe−NO complexes) have His residues with the H-δ interacting with strong negative groups (typically a carbonyl group as in the globins or a carboxylate moiety as in HRP). In the X-ray structures of AXCP (PDB codes 1E83, 1E84, 1E85, and 1E86), the His H-δ is either interacting with a water molecule (Figure 1) or with a CO molecule (in the CO bound structure).[20] Clearly, the structural data support the fact that AXCP has a neutral proximal His as the Fe ligand. It is interesting to note that both interpolations of AXCP-ν_{Fe-His} (209 and 214 cm^{-1}, taken from the linear regressions in Figure 2) are in good agreement for what is expected for a neutral His residue, and therefore a weak bond, characteristic of proteins that like AXCP, Fix-L, or sGC, form 5c-NO adducts (with the Fe−His bond broken).

To explain the high Fe−His stretching frequency in AXCP, Andrew et al.[26] suggested that it may be due to the fact that in the 5c-His complex, His is deprotonated and that it becomes protonated upon NO binding. The protonation of His is required since Fe−His bond breaking is not feasible for a deprotonated His, due to the much stronger Fe−His bond present in that case. We calculated the proton affinity of the proximal His with (6c-His−Fe−NO complex) and without NO (5c-His complex). The corresponding values are 366 and 354 kcal/mol for the 6c-His−Fe−NO and the 5c-His−Fe complexes, respectively. These results indicate that protonation on the His in the 6c-His−Fe−NO complex is slightly more favorable than in the 5c-His complex. However, both values are quite high as compared, for example, with the solvated imidazole proton affinity of 294

(43) Enemark, J. H.; Feltham, R. D. *Coord. Chem. Rev.* **1974**, *13*, 339−406.

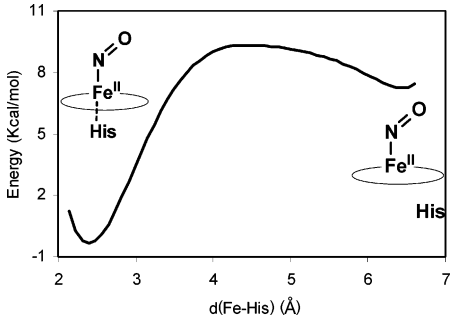

Figure 3. Energy vs reaction coordinate plot for the Fe−His bond breaking process. Energy in kcal/mol and Fe−His distance in Å.

kcal/mol, indicating that the His is likely to be neutral in both cases. Also, the estimates of ν_{Fe-His} for a negative His are too high ($\geq$240 cm^{-1}) (the estimate for the frequency is based on the ΔE and Δq values for an imidazolate ligand).[32] Taking this into consideration, the deprotonated His hypothesis seems unlikely. The high value of the Fe−His stretching frequency might be related to an internal Stark effect due to the positively polarized proximal environment caused by the presence of Arg 124 close to the proximal His 120.[44]

To further analyze the mechanism and energetics of Fe−His bond breaking, we performed a calculation of the energy profile of the Fe−His bond breaking reaction for the 6c complex with NO in the distal side of the heme. The chosen reaction coordinate was the Fe−Nϵ_{His} distance (see Figure 1). Figure 3 shows the corresponding energetic profile.

From the energetic reaction profile, the most interesting facts are the existence of the second local minimum corresponding to the 5c-NO complex and the low barrier (only 2 kcal/mol) for His rebinding. The existence of the second local minimum favors Fe−His bond breaking because the absence of another stable conformation would leave the His associated to the heme no matter how weak the bond is. In fact, the majority of heme proteins do form stable 6c-NO complexes due to the tendency of the protein matrix to hold the proximal His ligand. Evidence of an alternative conformation with the His detached from the heme has also been observed in the X-ray structure of quaternary nitrosyl Hb, in both α-chains. In this case, the 5c-NO complex presents the His rotated 180° about the $C_\beta-C_\gamma$ bond with respect to the NO free 5c-His complex.[45]

From Figure 3 and the corresponding structures along the reaction coordinate, the transition state (TS) (the point along the path with the maximum potential energy) can be identified. In the Fe−His bond breaking process, the TS structure presents an almost broken Fe−His bond (the Fe−His distance is 4.3 Å) and the His lying too close to Arg 124. Relaxing the structure to accommodate the His−Arg interaction drives the protein to the other minimum. To understand the molecular basis for the existence of the unbound minimum energy conformation, we have computed the interaction energy of His120 with Arg 124 by performing single point calculations of the interacting and isolated residues. As expected, the computed interaction energy is significant and negative, −9.5 kcal/mol, suggesting that this interaction plays a fundamental role in stabilizing the 5c-NO

(44) (a) Park, E. S.; Thomas, M. R.; Boxer, S. G. *J. Am. Chem. Soc.* **2000**, *122*, 12297−12303. (b) Suydam, I. T.; Boxer, S. G. *Biochemistry* **2003**, *42*, 12050−12055.

(45) Chan, N. L.; Kavanaugh, J. S.; Rogers, P. H.; Arnone, A. *Biochemistry* **2004**, *43*, 118−132.

Table 2. Proximal versus Distal Conformation for 5c-NO Complexes[a]

	$\Delta E_{prox-dis}$ (kcal/mol)	Fe–N–O (deg)		q_{NO} (*e*)	
		dist	prox	dist	prox
WT	−11.8	140.6	143.1	−0.066	−0.070
Leu$_{16}$*x*Gly	−0.9	141.4	142.6	−0.058	−0.053
Arg$_{124}$*x*Gly	−10.5	140.6	143.3	−0.085	−0.013
Leu$_{16}$*x*Gly and Arg$_{124}$*x*Gly	2.5	141.7	143.6	−0.078	−0.015

[a] The q_{NO} is given in *e* and the Fe−N−O angles in deg. $\Delta E_{prox-dis}$ is the energy difference between proximal and distal conformation for the 5c-NO complex (kcal/mol) (a negative value means that the proximal conformation is more stable).

local minimum. In contrast to the change observed in the Hb α-chains in AXCP, the 5c-NO conformation presents the His rotated nearly 90° around the $C_\alpha-C_\beta$ bond with respect to the 5c-His complex.

The low barrier (2 kcal/mol) and negative ΔE (−7.2 kcal/mol) for His rebinding would drive the His mainly to the bound state. The binding of a second NO molecule to the proximal site may, however, avoid His rebinding by trapping the protein in the 5c-NO proximal conformation.

Proximal versus Distal Conformation in the 5c-NO Complex. The experimental X-ray results for the 5c-NO complex show the NO present at the proximal side. The preference for this configuration has been attributed to the stabilizing interaction of Arg 124 on the NO; however, the sterical strain induced on NO by Leu 16 on the distal side cannot be discarded. To identify the contribution of these two factors on the NO configuration preference, we calculated the energy difference ($\Delta E_{prox-dis}$) between both configurations by performing QM-MM optimizations of complexes with NO in the proximal and distal sides of the heme. In all cases, both proximal and distal complexes turned out to be local minimum. We have performed QM-MM optimizations for the wild type (WT) enzyme, for the mutants Leu16$_x$Gly (leucine 16 residue in the WT protein replaced by a glycine residue), Arg124$_x$Gly (the arginine 124 residue of the WT protein replaced by a glycine residue), and the double mutant Leu16$_x$Gly and Arg124$_x$Gly (both leucine 16 and arginine 124 residues have been replaced by glycine residues). Additional details about the in silico constructed proteins may be found in the Supporting Information. In all cases, both coordination structures turned out to be local minima. The results for the relative energies and relevant structural parameters are presented in Table 2.

The results presented in Table 2 corroborate the experimentally observed fact that in AXCP the NO is more stable in the proximal position. The results also show that in the double mutant the preference is inverted, being more stable the distal configuration. The double mutant would represent a protein with both the distal and the proximal cavities almost free of residues that can stabilize/destabilize the coordinated ligands. Addition of an Arg124 residue to the double mutant in the proximal side (Leu16$_x$Gly protein) reverts the preference due to a stabilizing interaction between the Arg 124 and the proximal NO; however, the stabilization is small (−0.9 kcal/mol). On the other hand, addition of the Leu 16 residue in the distal cavity (Arg124$_x$Gly protein) stabilizes the proximal conformation by 10.5 kcal/mol, a value that is almost equal to the WT protein value. The results of Table 2 suggest that the proximal preference for NO is mainly due to the steric destabilization of Leu 16 and not because of

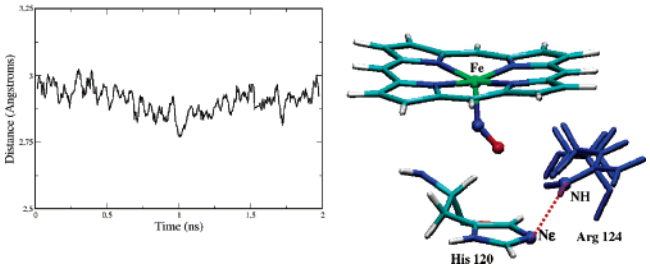

Figure 4. Time evolution of the Nϵ (His120)−NH(Arg124) distance.

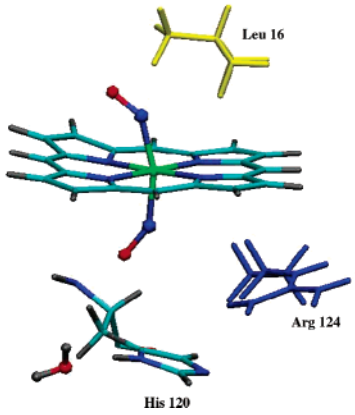

Figure 5. 6c-di-NO complex in AXCP.

the positive interaction with Arg 124. The small effect of Arg 124 stabilization can also be seen in the total NO charge that becomes slightly more negative (an indication of a higher degree of π back-donation) in the proximal conformation when Arg 124 is present.

To assess the role of the protein dynamics on the structure of the NO complexes, we have performed 2 ns of classical molecular dynamics simulations for the proximal and distal coordinated NO complexes in the WT protein. Inspection of the fluctuations of His 120 and Arg 124 (Figure 4) revealed that these amino acids interact favorably along the whole trajectory, maintaining an H bond between Nϵ (His 120) and NH (Arg 124) (Figure 4). This suggests that this interaction plays an important role stabilizing the His away from the heme. Interestingly, we also found that His 120 remains away from the heme in the simulation time scale also in the case in which NO is bound to the distal side of the heme (data not shown), corroborating that the conformation with His detached from the heme is indeed a local minimum.

Structural Characteristics of the 6c-di-NO Complex in AXCP. We have analyzed also the likelihood of the existence of a transient 6c-di-NO intermediate, motivated by the fact that an Fe(II) porphyrinate 6c-di-NO complex has already been characterized theoretically by means of DFT calculations[46] and that experimental results for the model system Fe(II)-meso-tetrakis-phenyl-porphyrinate-di NO have also been recently reported.[47]

To have a final conformation with NO bound at the proximal side, one possibility is that a second NO molecule binds to the 5c-NO complex at the now vacant proximal side. Figure 5 shows the corresponding QM-MM optimized structure in AXCP.

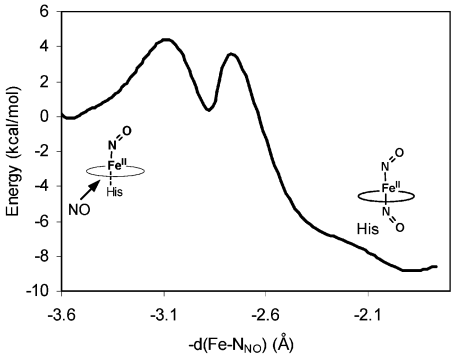

Figure 6. Energy vs reaction coordinate plot for NO attack to the 6c-NO complex.

The 6c-di-NO complex has two possible conformations, cis and trans (in the cis conformation nitrosyl oxygens are oriented in the same direction, whereas in the trans conformation, they are oriented in opposite directions). Previous DFT calculations for a porphyrin model (without the heme side chains) showed that the complex is low spin and that the cis conformation is favored.[46] Our results for the same model in a vacuum confirm this fact, showing a difference of 4.7 kcal/mol between both conformations. In the AXCP protein, the QM-MM optimized 6c-di-NO complex in the cis conformation has the distal NO pointing away from Leu 16 and the proximal NO pointing away from Arg 124 (see Figure 5).

After the distal NO is released, the proximal NO probably rotates to interact with Arg 124 adopting the final conformation observed in the X-ray structures. The affinity of the AXCP protein for the second (proximal) NO is lower as compared to the first (distal) NO (−18.5 vs −42.3 kcal/mol). In vacuum for a heme model without side chains, the affinity for the second NO is also lower than for the first NO (−21.6 vs −47.6 kcal/mol). These data corroborate that the 6c-di-NO complexes are less stable than the 5c-NO complexes. The short-lived nature of 6c-di-NO complexes has been established in the work by Lorkovic et al.[47] These authors obtained them only at low temperatures (179 K). No appreciable formation of the 6c-di-NO complex was observed at 295 K. On the other hand, 5c-NO complexes are known to be very stable at room temperature. It is also interesting to note that in the 6c-di-NO complex, both proximal and distal NO molecules have significantly different dissociation energy barriers to go from the 6c-di-NO to the 5c-NO complexes. For the formation of the 5c-NO proximal complex (the final complex observed in the X-ray structure), the energy barrier is only 6.7 kcal/mol, as compared with a value of 18.5 kcal/mol for the 5c-NO distal complex. These results corroborate that the final 5c-NO complex is likely to present the NO located on the proximal site.

Direct Attack of a Second NO to the 6c-NO Complex. Another possibility to yield the 6c-di-NO complex is a direct attack of a second NO molecule to the initial 6c-His−Fe−NO complex. Then, the concerted formation of the Fe−NO bond and rupture of the Fe−His bond would yield the 6c-di-NO complex. To analyze this possibility, we computed the energy profile for the corresponding reaction in the protein. The chosen reaction coordinate was the Fe−N distance for the second NO molecule, which attacks Fe from the proximal side of the heme. The corresponding energy profile is presented in Figure 6.

(46) Conradie, J.; Wondimagegn, T.; Ghosh, A. *J. Am. Chem. Soc.* **2003**, *125*, 4968−4969.
(47) (a) Lorkovic, I.; Ford, P. C. *J. Am. Chem. Soc.* **2000**, *122*, 6516−6517. (b) Ford, P. C.; Lorkovic, I. *Chem. Rev.* **2002**, *102*, 993−1017.

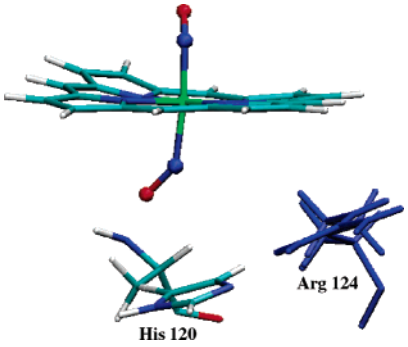

Figure 7. 6c-di-NO local minimum intermediate in AXCP.

Scheme 2. Proposed Mechanism for NO Interaction with AXCP[a]

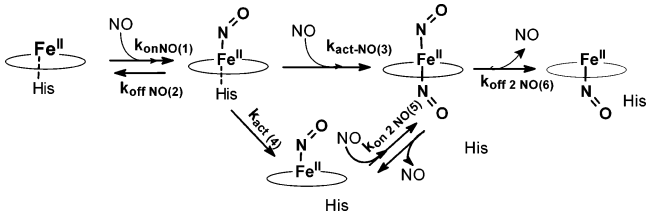

[a] In the conversion of the 6c species to the 5c-NO heme complex, NO first displaces the His yielding the 6c-di-NO complex (reaction 3). Reaction 4 does not involve NO and represents the breaking of the Fe−His bond. Reactions 5 and 6 are the binding and release of the second NO once the Fe−His bond is broken.

The profile shows that there are two small barriers separated by an intermediate (local minimum), depicted in Figure 7. The first barrier of 4 kcal/mol is associated with the breaking of the Fe−His bond and the formation of the Fe−NO bond, forming an intermediate complex that exhibits an Fe− NO bond, but with an almost broken Fe−His bond (the Fe−His distance is 5.45 Å) and the His lying too close to Arg 124 (Figure 7). The second barrier is lower (3 kcal/mol with respect to the intermediate local minimum conformation) and corresponds to the process of relaxing the His, to allow it to interact favorably with Arg 124 as in the final 6c-di-NO complex (compare Figures 5 and 7). It is also noteworthy that the intermediate local minimum exhibits the NO in a stereochemically hindered conformation due to the presence of the nearby His. Relaxing of this conformation also contributes to the low energy of the final resulting 6c-di-NO complex. Another interesting fact is that in this case, the barrier for His rebinding once the final conformation is reached is significant.

Andrew et al. proposed that His reattachment facilitates NO release following photochemical or thermal NO dissociation.[27] The authors hypothesized that this mechanism termed kinetic trap could also be operative in NO-activated sGC and promote sGC deactivation.[27] One of the fundamental questions on sGC is how the high affinity for NO is overcome to deactivate the enzyme.[27,49] As can be seen in Figure 3, when the proximal site is vacant, the barrier for His rebinding is very small. The resulting 5c-His complex would block the proximal site for NO. This is consistent with the hypothesis by Andrew et al. that fast His reattachment would avoid NO recombination, a process that is known to be very fast for vacant Fe binding sites.[27]

Taken together, these results support the mechanism presented by Marletta's group (Scheme 1), assuming that the results for AXCP can be generalized to sGC. We find that for AXCP, all steps involved in the Scheme 1 mechanism are feasible. In particular, our results show that the NO independent (reaction 4) and NO dependent (reaction 3) activation mechanism (6c-NO to 5c-NO switch) are both thermodynamically and kinetically feasible (Figure 3 and Table 2). The results also show that the possibility of 6c-NO to 5c-NO conversion in a particular heme protein will depend on two factors. In the first place, it will depend on a labile Fe−His bond (which is evidenced in sGC by the low ν_{Fe-His} of 204 cm^{-1}), and second, the existence of another local minimum 5c-NO conformation with the His detached from the heme. In the case of AXCP, the 5c-NO conformation is stabilized by the presence of Arg 124, which favorably interacts with the His. In the case of the NO dependent activation mechanism (reaction 3), the rate will also depend on the accessibility of NO to the proximal side.

Our results for AXCP point to an even more complex mechanism for this protein than that shown in Scheme 1, which takes into account the transient 6c-diNO complex. The proposed complete model is shown in Scheme 2.

The role of the second NO molecule as a catalyst in the activation mechanism of sGC can be assessed by performing the following analysis of the available experimental rate constants. In AXCP, the NO dependent rate constant (k_{act-NO}) for the 6c-NO to 5c-NO conversion has been experimentally determined, yielding values of 3.3×10^3 and 8.1×10^3 M^{-1} s^{-1}.[26,27] Both values are smaller than the corresponding one for sGC obtained by Marletta's group (2.4×10^5 M^{-1} s^{-1}).[13,14]

The rate constant for the uncatalyzed 6c-NO to 5c-NO in AXCP is not known. However, the reported values for the k_{act-NO} in AXCP are still more than 3 orders of magnitude larger than both rate constant estimated values for the uncatalyzed 6c-NO to 5c-NO conversion in sGC (5×10^{-4}[13,14] and 1.3 s^{-1}[15]).

Our QM-MM calculations provide useful comparative energetic information regarding both the catalyzed and the uncatalyzed reactions (Figures 3 and 6). Our results for the energy barriers for the NO catalyzed (reaction 3) and uncatalyzed (reaction 4) activation steps are 4.0 and 9.2 kcal/mol, respectively. The uncatalyzed reaction rate depends only on the amount of 6c-NO protein. On the other hand, the catalyzed reaction is a second-order reaction that depends also on the NO concentration. The computed reaction profile (Figure 6) assumes that NO is already present in the active site, and so NO diffusion into the protein is not considered. This would be the case in NO saturating concentrations.

On the basis of these assumptions, the computed energetic barriers yield an estimate of about 3 orders of magnitude for the NO-catalyzed/NO-uncatalyzed 6c-NO to 5c-NO conversion rates ratio for AXCP. At lower NO concentrations, the NO-catalyzed/NO-uncatalyzed 6c-NO to 5c-NO conversion rates ratio is expected to decrease.

Finally, it is interesting to note that the real rate of sGC activation will depend on which mechanism is operative. The uncatalyzed activation rate depends only on k_{act} and the amount of 6c-NO complex, whereas the NO catalyzed activation rate depends on k_{act-NO}, the amount of 6c-NO, and also the NO concentration. The upper limit for the physiological NO concentration is in the micromolar range ([NO] < 1 μM).[48]

(48) (a) Malinski, T.; Czuchajowski, C. *Methods in Nitric Oxide Research*; Feelish, M., Stamler, J. S., Eds.; J. Wiley and Sons: Cichester, UK, 1996; Ch. 6 and references therein. (b) Hirota, Y.; Ishida, H.; Genka, C.; Obama, R.; Matsuyama, S.; Nakasawa, H. *Jpn. J. Physiol.* **2001**, *51*, 455−461.
(49) Condorelli, P.; George, S. C. *Biophys. J.* **2001**, *80*, 2110−2119.

Table 3. Oxygen Affinity Energy Values (kcal/mol)[a]

	ΔE (kcal/mol)	q_{O2} (e)	Δq_{His} (e)
WT	8.4	−0.262	0.124
Leu_{16}/Gly	23.3	−0.231	0.106
heme	21.4	−0.202	0.158
TrHbN	37.2	− 0.360	0.210

[a] Δq_{His} and Δq_{O2} (e) are the computed charges received and donated by the oxygen and His ligands, respectively.

However, in vivo studies of sGC activation showed that NO can control sGC in the range of 1−100 nM.[49] For [NO] = 100 nM, sGC−NO formation rate would be about 10 × [sGC] s^{-1}, and the 6c-NO to 5c-NO conversion rates would be 2.4×10^{-2} × [sGC−NO] s^{-1} for the NO catalyzed conversion and 5×10^{-4} × [sGC−NO] s^{-1} for the uncatalyzed conversion (rate constants obtained from refs 13 and 14, mentioned previously). In this scenario, clearly sGC−NO accumulates (the initial 6c-NO to 5c-NO conversion rate is around 400 times slower than sGC−NO formation even at equal concentrations of sGC and sGC−NO). Therefore, sGC is activated mainly by the NO catalyzed mechanism (the ratio NO-catalyzed/NO-uncatalyzed conversion rates is 48). However, for [NO] = 1 nM, the sGC−NO formation rate is only 0.1 × [sGC] s^{-1}, and the 6c-NO to 5c-NO conversion rates are 2.4×10^{-4} × [sGC−NO] s^{-1} for the NO catalyzed conversion and 5×10^{-4} × [sGC−NO] s^{-1} for the uncatalyzed conversion. In this scenario, sGC−NO also accumulates but at a 1000 times slower rate, and it is activated both by NO uncatalyzed and catalyzed pathways (the ratio NO-catalyzed/NO-uncatalyzed conversion rates is 0.48). These results show that for high NO concentrations (about 100 nM), the sGC activation rate is doubly enhanced because there is an increase in the rate of 6c-NO complex formation, and also the 6c-NO to 5c-NO conversion rate increases through the NO catalyzed pathway.

Oxygen Affinity in AXCP. We mentioned previously that another similarity between AXCP and sGC is that none of them bind oxygen. To explore the molecular basis for this fact, we calculated the oxygen affinity of WT AXCP and the $Leu16_x$-Gly mutant. Table 3 shows the oxygen affinity for the WT, the mutant protein, and an isolated heme model system (without the protein side chains). The calculated oxygen affinity of truncated hemoglobin N (TrHbN) of *Mycobacterium tuberculosis* (a globin with a high oxygen affinity calculated with the same method) is also shown for comparison.[50]

As can be seen from Table 3, the oxygen affinity is very low in WT AXCP, even lower than in the heme model system. The mutation of $Leu16_x$Gly reverts partially this effect, yielding a value that is similar to that of the model system. However, the affinity is still low as compared to proteins such as TrHbN that bind oxygen strongly, primarily because of distal stabilization of the bound oxygen through H-bond interactions. AXCP does not present any H-bond donor group in the distal side; therefore, even in $Leu16_x$GLY, the oxygen affinity is moderate.

6c-His-Fe−CO Complex in AXCP. Another interesting characteristic mentioned previously is the fact that in the X-ray structures of AXCP, CO is found on the distal side, whereas NO is found bound to the proximal side of the heme. We computed the 6c His-Fe−CO complex in AXCP and as expected, a positive trans effect was found.[51] (The Fe−His distance is 2.11 Å in the CO complex, as compared to 2.18 Å in the 5c-His complex.) The CO binding energy of 48.0 kcal/mol is similar to that found for NO (42.3 kcal/mol) and significantly larger than that of O_2 (8.4 kcal/ mol). The distinct binding pattern for the three diatomic ligands can be understood in terms of the intrinsic binding properties of the ligands to the heme, possible distal interactions, and proximal trans effects. The hydrophobic crowded distal pocket inhibits oxygen binding. Typically, oxygen complexes in heme proteins display hydrogen bonding donor groups in the distal side that stabilize the negatively bound oxygen through H-bond interactions.[50] On the other hand, NO and CO bind more tightly to the iron and do not require further distal stabilization to form the corresponding 6c complexes. In the CO adduct, the positive trans effect reinforces the Fe−His bond, and the His remains tightly bound to the heme, blocking the proximal position and leaving the CO with only the distal coordination possibility. On the contrary, the NO negative trans effect weakens the Fe−His bond. The His residue is then displaced by another NO molecule that binds to the proximal side. The NO proximal preference (see Table 2) drives the protein to the finally observed 5c Fe−NO (proximal) configuration, as experimentally determined.

AXCP provides a good model for understanding NO, CO, and O_2 interactions with heme proteins. Given the two distinct distal resting states and environments reported so far for sGC, the use of AXCP as a model for sGC would be representative of sGC_2, which displays a high spin 5c-His−Fe resting state. However, AXCP exhibits a hydrophobic distal pocket, similar to that proposed for sGC1 on the basis of spectroscopic measurements of the sGC_1−CO adduct.[4,5] A more detailed comparison between AXCP and sGC interaction with small ligands awaits confirmation of the distal pocket characteristics of sGC. In any case, the results presented here support Marletta's model of sGC activation in which NO acts not only as the iron ligand but also catalyzes the activation step. Our results also show that the preference in the position of NO (distal or proximal) in the final 5c-NO in AXCP is determined mainly by the presence of Leu 16 that occludes the distal position. Also, this causes AXCP not to bind O_2. If the same reason prevents oxygen binding to sGC remains to be proven.

Acknowledgment. Prof. J. A. Olabe is kindly acknowledged for many valuable suggestions. This work was partially supported by the University of Buenos Aires, Agencia Nacional de Promoción Científica y Tecnológica (project PICT 06-08447), CONICET (PIP 02508), and Fundación Antorchas.

Supporting Information Available: Optimized structures for active sites in PDB format and additional computational methodology information. This material is available free of charge via Internet at http://pubs.acs.org.

JA042870C

(50) (a) Milani, M.; Pesce, A.; Nardini, M.; Ouellet, H.; Ouellet, Y.; Dewilde, S.; Bocedi, A.; Ascenzi, P.; Guertin, M.; Moens, L.; Friedman, J. M.; Wittemberg, J. B.; Bolognesi, M. *J. Inorg. Biochem.* **2005**, *99*, 97−109. (b) Crespo, A.; Martí, M. A.; Kalko, S. G.; Morreale, A.; Orozco, M.; Gelpi, J. L.; Luque, F. J.; Estrin, D. *J. Am. Chem. Soc.* **2005**, *127*, 4433−4444.

(51) Traylor, T. G.; Sharma, V. S. *Biochemistry* **1992**, *31*, 2847−2849.